International Journal of Pharmaceutics 416 (2011) 25–34

Contents lists available at ScienceDirect

International Journal of Pharmaceutics

journal homepage: www.elsevier.com/locate/ijpharm

A method for the aerodynamic design of dry powder inhalers

Ö. Ertunç[a,b,*], Ç. Köksoy[a], H. Wachtel[c], A. Delgado[a,b]

[a] Institute of Fluid Mechanics, Friedrich-Alexander-University Erlangen-Nuremberg Cauerstrasse 4, D-91058 Erlangen, Germany
[b] Erlangen Graduate School of Advanced Optical Technologies (SAOT), Germany
[c] Boehringer Ingelheim Pharma GmbH & Co. KG, Ingelheim, Germany

ARTICLE INFO

Article history:
Received 17 January 2011
Received in revised form 17 May 2011
Accepted 18 May 2011
Available online 28 June 2011

Keywords:
DPI
Dry powder
Inhaler
Fluid mechanics
Design
Flow visualization

ABSTRACT

An inhaler design methodology was developed and then used to design a new dry powder inhaler (DPI) which aimed to fulfill two main performance requirements. The first requirement was that the patient should be able to completely empty the dry powder from the blister in which it is stored by inspiratory effort alone. The second requirement was that the flow resistance of the inhaler should be geared to optimum patient comfort. The emptying of a blister is a two-phase flow problem, whilst the adjustment of the flow resistance is an aerodynamic design problem. The core of the method comprised visualization of fluid and particle flow in upscaled prototypes operated in water. The prototypes and particles were upscaled so that dynamic similarity conditions were approximated as closely as possible. The initial step in the design method was to characterize different blister prototypes by measurements of their flow resistance and particle emptying performance. The blisters were then compared with regard to their aerodynamic performance and their ease of production. Following selection of candidate blisters, the other components such as needle, bypass and mouthpiece were dimensioned on the basis of node-loop operations and validation experiments. The final shape of the inhaler was achieved by experimental iteration.

1. Introduction

Dry powder inhalers (DPIs) are used to deliver drugs by the pulmonary route. Many DPIs are designed for the topical treatment of respiratory diseases (Chodosh et al., 2001) but some are intended to deliver drugs for a systemic effect, providing alternative options for the administration of macroproteins, hormones (Patton et al., 1994), paediatric vaccines (Licalsi et al., 1999) and insulin (Owens et al., 2003) etc. All these new developments increase the need for consistent drug dosing. A variety of different dosing systems have been used in DPIs (Ashurst et al., 2000). The most common method has been to fill a specific quantity of the drug powder into a blister or capsule. For any new DPI of this design, complete emptying of the blister or capsule is necessary to ensure consistent drug delivery with each actuation. Multidose systems generally employ blister structures owing to their ease of use. In these systems, blister cavities are located in such a way that a mechanism opens the protective foil of one cavity and then moves the cavity to a position where its contents (powder particles) are emptied for delivery to the patient.

Emptying of the blister is achieved either by the patient's inspiratory effort or by another mechanism which provides energy for powder dispersion and which is activated, directly or indirectly, by the patient. DPIs relying on the patient's inspiratory effort alone are called passive DPIs and DPIs employing another mechanism are called active DPIs (Islam and Gladki, 2008). In both types of DPI, the inhaler should be able to disperse the drug powder, which is mostly in the agglomerated state, in such a way that smaller active particles can reach the alveoli whilst the patient is inhaling (Breuer et al., 2006, 2007).

The focus of this work is the aerodynamic design of a multidose passive DPI. A design method is proposed to fulfill the requirements for complete emptying of the blisters and for the flow resistance experienced by the patient. The emptying of a blister is a two-phase flow problem, whilst the adjustment of the flow resistance to optimize patient comfort is an aerodynamic design problem. A design method has therefore been developed which simultaneously addresses the two-phase flow problem and the aerodynamic design problem. The proposed method relies heavily on fluid/particle flow visualization and pressure drop measurements in inhaler prototypes. Using the dynamic similarity concept (Wachtel et al., 2008), most of the experimental work was conducted in a water channel with upscaled models of inhalers and particles. Real-scale emptying experiments were conducted for only a few selected blister prototypes. Another important component of the proposed design is the application of node-loop

* Corresponding author at: Institute of Fluid Mechanics, Friedrich-Alexander-University Erlangen-Nuremberg Cauerstrasse 4, D-91058 Erlangen, Germany. Tel.: +49 9131 8529472, fax: +49 9131 8529503.
E-mail address: ertunc@lstm.uni-erlangen.de (Ö. Ertunç).
URL: http://www.lstm.uni-erlangen.de (Ö. Ertunç).

0378-5173/$ – see front matter © 2011 Elsevier B.V. All rights reserved.
doi:10.1016/j.ijpharm.2011.05.045

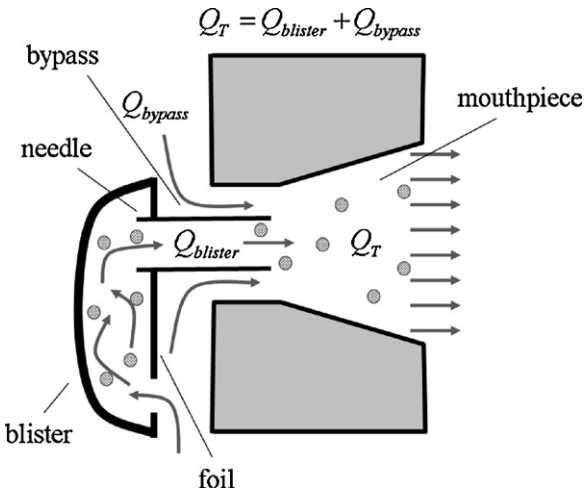

Fig. 1. Sketch of the selected DPI configuration which is subjected to further design and optimization in the present study.

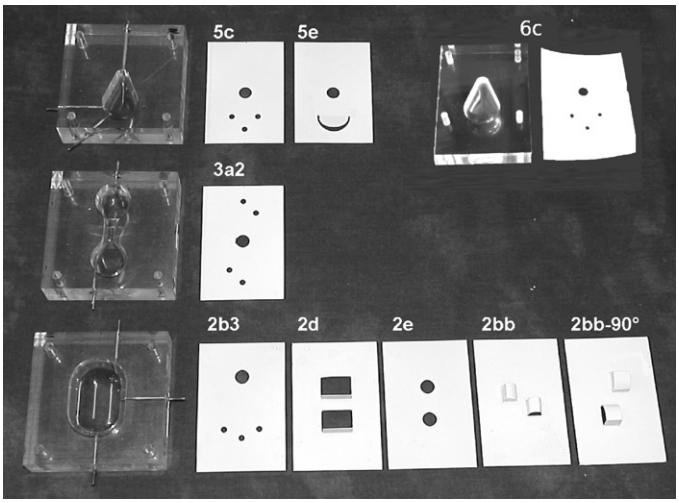

Fig. 2. Blisters and lid foils tested.

operations (Larock et al., 1999) to dimension the various components of the inhaler.

The theoretical and experimental description of the design method is accompanied throughout the paper by the actual design of a specimen DPI, referred to henceforth as the "new DPI". Section 2.1 of the paper provides an overview of the design method. Section 2.2 addresses dynamic similarity considerations related to flow in the inhaler and two-phase flow and also provides theoretical background to the dimensional analysis and the node-loop operations. Section 2.3 comprises a description of the experimental set-up and measurement procedures. In Section 3.1, the blister cavities are characterized. Optimization and finalization of the design of the new DPI within the relevant constraints is explained in Section 3.2. Section 4 summarizes the conclusions and future perspectives.

2. Materials and methods

2.1. Overview of the design method

By following steps 1–7 below, an inhaler satisfying common performance requirements on emptying and flow resistance can be designed.

Step 1: The design and optimization process starts with the conceptual design of the inhaler. The design shown in Fig. 1 is selected as the initial basis for optimization work. In this design, the blister is filled with the drug in powder form and the drug is inhaled by the patient through the needle and mouthpiece. A bypass opening helps to reduce the flow resistance experienced by the patient.

Step 2: The performance requirements should be determined. In the present study, the new DPI must meet the following requirements:

- The flow resistance characteristics should resemble those of the HandiHaler® (Boehringer Ingelheim Pharma GmbH & Co. KG), creating a pressure drop of 4 kPa at 39 l/min and 1 kPa at 20 l/min (de Boer et al., 1996).
- In the present design concept, the blister should be completely emptied at a flow rate of 20 l/min. A flow rate of 20 l/min and a pressure drop of 1 kPa represent values which can be achieved even by patients with severe airflow limitation (Chodosh et al., 2001).

Step 3: The configuration of the blister cavity and the configuration of the inlet and exit holes on the lid foil plays a crucial role in blister emptying. Hence, as a third step of the design method, conceptual designs of blisters and lid foils must be developed. The selected blister cavity and lid foil configurations are shown in Fig. 2.

Step 4: The performance of the candidate blisters is quantified in terms of (a) the flow rate at which complete emptying of particles from the blister is achieved and (b) the flow resistance of the blisters. Further evaluations must now be made regarding ease of production, patent issues etc. The number of candidate blisters can be reduced at this stage.

Step 5: The flow resistances of the other components such as the needle, bypass and mouthpiece are measured.

Step 6: The inhaler design can now be compared against the requirements specified in step 2. The flow resistance of the initial design can be approximated using node-loop operations and the flow resistance coefficients can be determined from pressure drop measurements across each component of the inhaler. At this stage, tests can be carried out to determine whether the selected blister can be fully emptied within the operating range of the inhaler.

If the requirements are not met, target values for flow resistance coefficients for each component are determined using node-loop operations so that the inhaler can satisfy the two requirements specified in step 2.

Step 7: All components are dimensioned to attain the values specified in step 6. After a number of dimensioning iterations and measurements have been carried out, the final inhaler shape is achieved. Finalized inhaler configurations are now ready to be tested under real conditions.

2.2. Analytical considerations

2.2.1. Dimensional analysis and dynamic similitude

In current DPIs, air flow may locally reach velocities in the order of 100 m/s. Detailed visual investigation of flow at such high velocities is very cumbersome and extremely impractical owing to the small dimensions of the devices. It is therefore common practice to conduct experiments with upscaled models in other fluids such that the flow in the model shows geometric, kinematic and dynamic similarity to the flow in and/or around the actual equipment. When designing model experiments of this type, it is important to ensure that dimensionless numbers quantifying different physical effects on the phenomena investigated are consistent between the actual device and the model. In the present study, Reynolds number (Re) and Archimedes number (Ar) similarities are employed for flow

visualization, pressure drop and particle emptying experiments. The *Re* for flow in the DPI is defined as:

$$Re = \frac{UL}{\nu} \tag{1}$$

where U, L and ν are characteristic velocity in DPI, characteristic length of DPI and kinematic viscosity of the carrier fluid respectively. The inhaler can be geometrically upscaled by the factor F:

$$L_m = FL_a \tag{2}$$

where L_m and L_a are characteristic dimensions of the upscaled model of the inhaler and the actual inhaler, respectively. In the subsequent text, the subscript m and a denote the operation of the model inhaler with model fluid and the actual inhaler with actual carrier fluid (air) respectively. By keeping *Re* constant, the velocity and flow rate relationships for model and actual operations of the inhaler can be defined as follows:

$$U_a = U_m F \frac{\nu_a}{\nu_m} \tag{3a}$$

$$Q_a = Q_m \frac{1}{F} \frac{\nu_a}{\nu_m} \tag{3b}$$

As the flow in upscaled and actual inhalers are dynamically similar, the pressure drop measured in one can be converted to the other. In order to convert upscaled measurements to the actual inhaler, measured pressure drop values must be normalized by the dynamic pressure:

$$C_p = \frac{\Delta P}{(1/2)\rho_f U^2} \tag{4}$$

C_p, the so called non-dimensional pressure drop coefficient and ρ_f is the density of the carrier fluid. Thus, the following equality holds

$$C_p = \frac{\Delta P_m}{(1/2)\rho_m U_m^2} = \frac{\Delta P_a}{(1/2)\rho_a U_a^2} \tag{5}$$

from which one can write with the help of Eq. (3a)

$$\Delta P_a = \Delta P_m F^2 \frac{\rho_a}{\rho_m} \left(\frac{\nu_a}{\nu_m}\right)^2. \tag{6}$$

According to Kalman et al. (2005), the pickup of particles from the horizontal walls of channels and pipes is a function of the particle Reynolds number Re_p and the Archimedes number Ar:

$$Re_p = \frac{Ud_p}{\nu} \tag{7a}$$

$$Ar = \frac{gd_p^3}{\nu^2} \frac{\rho_p - \rho_f}{\rho_f} \tag{7b}$$

where d_p and ρ_p are the diameter and the density of the particles respectively. The critical pickup velocity of particles (U_p^*) in channels and pipes can be obtained from the empirical functions of particle Reynolds number (Re_p^*) and Archimedes number (Ar), which are given in Fig. 3. Re_p^* is defined with the fluid velocity at which particles are picked up from the surface:

$$Re_p^* = \frac{U_p^* d_p}{\nu} \tag{8}$$

In order to perform representative experiments of particle emptying from blisters, Re_p and Ar should also be kept constant in the experiments performed with upscaled inhaler components. The *Re* similarity used in the upscaled experiments dictates the velocity relationship (3a); consequently, in order to maintain *Re* similarity at the particle level, the ratio of the particle diameters used in the experiments should be upscaled as follows:

$$d_{p_m} = Fd_{p_a}. \tag{9}$$

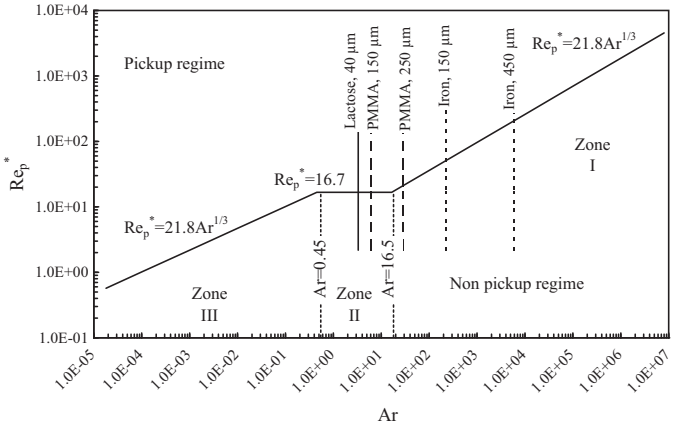

Fig. 3. Three zones model of Kalman et al. (2005) showing the pickup *Re* number in channels and pipes as a function of *Ar* number.

In order to have full similarity of the two-phase flow, the Archimedes number should also be kept the constant, hence the particles used have the following density

$$\rho_{p_m} = \rho_m + \frac{1}{F^3} \frac{\nu_m^2}{\nu_a^2} \frac{\rho_m}{\rho_a} (\rho_{p_a} - \rho_a). \tag{10}$$

In the actual DPI 40 μm non-spherical lactose particles having 1540 kg/m^3 density are used together with air as the carrier fluid. For visualization experiments, 5 times upscaled geometrically similar models ($F = 5$) were constructed and water was used as carrier fluid. Inserting, the physical properties of carrier fluid, particles and the scaling factor in to the equations above, the following conversion factors can be found for full dynamic similarity:

$$d_{p_{air}} = 0.2 d_{p_{water}} \tag{11a}$$

$$U_{air} = 74.75 U_{water} \tag{11b}$$

$$Q_{air} = 2.99 Q_{water} \tag{11c}$$

$$\Delta P_{air} = 6.66\ \Delta P_{water} \tag{11d}$$

$$\rho_{p_{water}} = 1046\ \text{kg/m}^3 \tag{11e}$$

The overall effect is to increase the inhaler's dimensions and reduce the flow velocity by almost two orders of magnitude. Both of these factors ease the visualization of flow and particles.

Although the DPI can not be idealized as channel or pipe, scaling law for the pickup of particles from a wall (Kalman et al., 2005) (Fig. 3) can be utilized for guessing the order of magnitude of the pickup velocity (U_p^*). In the investigated DPI, the Ar number is 3.3 and it corresponds to the *zone II* in which the Re_p^* is constant and equal to 16.7. This finding suggests that by keeping the diameter of the model particle d_{p_m} around 200 micrometer, the density of the particles can be selected over a range between 1006 and 1215 kg/m^3. Selecting, particles having diameters larger than 200 micrometers with densities higher than 1215 kg/m^3 requires higher pickup velocities than necessary.

It is clear from Re_p^*–Ar plot (Fig. 3), in order to pick up the particles, particle Reynolds number, Re_p should be higher than the particle pick-up Reynolds number, Re_p^*, i.e.

$$Re_p > Re_p^*. \tag{12}$$

Hence, the higher the velocity in the blisters, the more complete emptying would be if Re_p lies in the pickup regime. It should be noted that the Re_p^*–Ar plot of Kalman et al. (2005) is valid only for flow conditions similar to those in pipes and channels. In contrast to the parallel flow found in pipes and channels, the velocity vector in blisters can have arbitrary directions and there can be

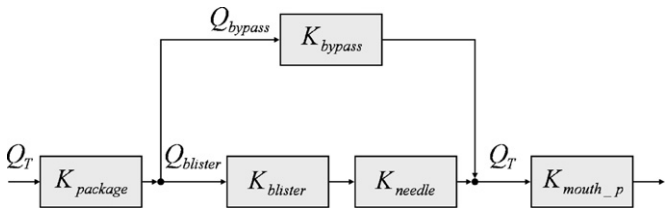

Fig. 4. Connection diagram for the components of the inhaler.

regions of circulation. Therefore, every blister has its own pickup characteristics.

The Re_p^*–Ar plot of Kalman et al. (2005) should only be used as a phantom map to guide experimentation and aid understanding. As the pickup Re_p^*–Ar of individual blisters is not known, experiments are required to judge whether complete emptying is possible in various blister models.

2.2.2. Flow resistance model of a DPI inhaler

The pressure drop across a passive flow machine can be approximated by linear function of the square of flow rate Q:

$$\Delta P = KQ^2. \tag{13}$$

The analogy of parallel- and serially connected resistances to fluid machines will be applied for the aerodynamic optimization of the inhaler components. When two passive flow machines are connected serially, they encounter the same flow rate and the resultant pressure drop is therefore the sum of the pressure drops across the two machines:

$$\Delta P_r = \Delta P_1 + \Delta P_2 \tag{14}$$

Thus, the resultant pressure resistance coefficient K_r reads

$$K_r = K_1 + K_2 \tag{15}$$

Where two flow machines are connected in parallel, the machines would encounter the same pressure drop but different flow rates. Using Eq. (13), the resultant pressure resistance coefficient K_r can be derived as:

$$K_r = \frac{K_1 K_2}{K_1 + K_2 + 2\sqrt{K_1 K_2}} \tag{16}$$

Following the path of the air, the basic DPI configuration in Fig. 1 can be modeled with the serial and parallel connections shown in Fig. 4. The bypass opening is in parallel to blister and the needle which are connected serially. The bypass + (blister + needle) is serially connected to the package and the mouth piece.

In order to adjust the overall flow resistance coefficient of the inhaler ($K_{inhaler}$), the contribution of each component to $K_{inhaler}$ must be formulated.

Using the Eqs. (15) and (16), the flow resistance coefficient of the inhaler can be written as:

$$K_{inhaler} = K_{package} + \frac{(K_{blister} + K_{needle})K_{bypass}}{K_{blister} + K_{needle} + K_{bypass} + 2\sqrt{(K_{blister} + K_{needle})K_{bypass}}} + K_{mouth\_p} \tag{17}$$

This equation suggests that any increase in the flow resistance coefficient of any component, causes an increase of $K_{inhaler}$, which results a drop in the flow rate through the DPI for a selected pressure drop. The bypass opening not only effects the flow resistance of the DPI, but also effects the flow rate that passes through the blister.

In the present study, the target $K_{inhaler}$ is 2.62 [Pa/(l/min)^2]. In addition, the blister should be completely emptied at the selected operating condition of ΔP = 1000 Pa and $Q_{inhaler}$ = 20 l/min. Thus, at the selected operating condition, the flow rate through the blister should be higher than the measured minimum flow rate required for emptying. In order to satisfy these requirements, the K values of the components should be adjusted appropriately. Using Eq. (17), all possible combinations of K values resulting in a $K_{inhaler}$ of 2.62 are calculated; the results are presented in Fig. 5. Each line in this figure, depicts the dependency of the K values of bypass, needle and blister at a constant value of $K_{package} + K_{mouth\_p}$.

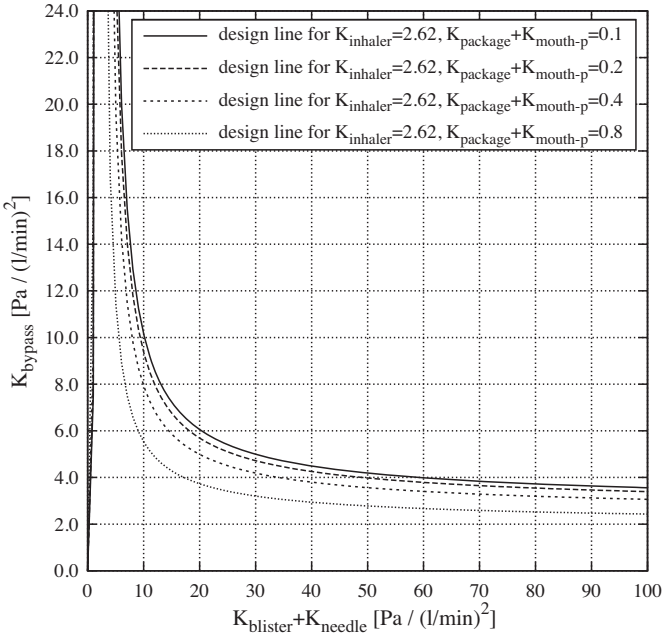

Fig. 5. The relationship between the K values of different components calculated for $K_{inhaler}$ = 2.62 by varying $K_{package} + K_{mouth_p}$.

The Eq. (17) together with Eq. (13) can be used to calculate the flow rate through the blister ($Q_{blister}$) as shown in Fig. 6. This calculation was carried out for an inhaler flow rate (Q_T) of 20 l/min (lowest flow rate constraint) on the assumption that $K_{package} + K_{mouth_p}$ = 0.1 [Pa/(l/min)^2]. The solid black line in Fig. 6 depicts the relation

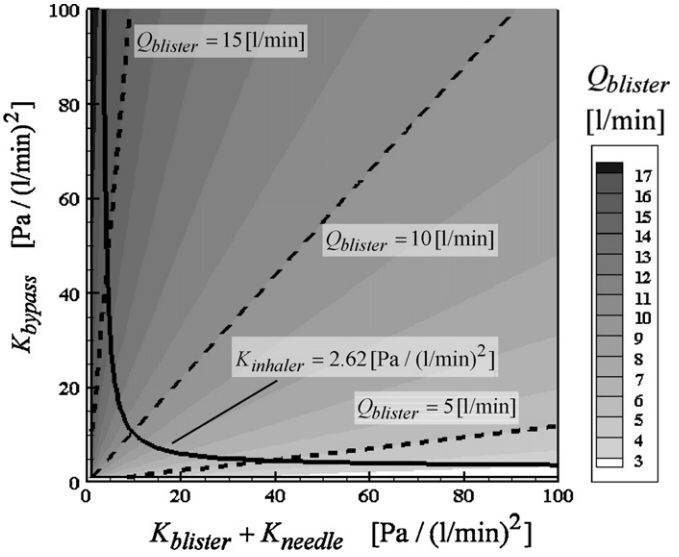

Fig. 6. The change of flow rate in the blister as a function of the K values of the components. Calculations are made on the assumption that $K_{package} + K_{mouth_p}$ = 0.1 [Pa/(l/min)^2] and Q_T = 20 [l/min].

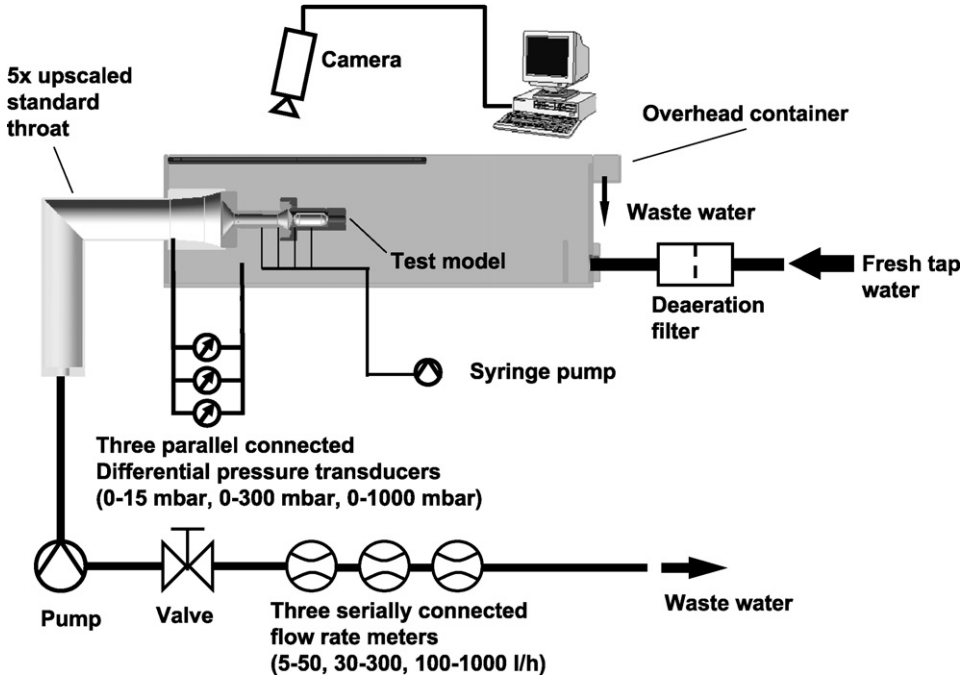

Fig. 7. Flow facility and instrumentation for the experiments with upscaled inhaler models.

between the K values of bypass, needle and blister (design line) and the contour plot shows the corresponding flow rate through blister, $Q_{blister}$.

In order to ensure complete emptying, the flow rate through the blister should be kept high, and this can easily be achieved if $K_{blister} + K_{needle}$ is kept low (Fig. 6). However, for very low values of $K_{blister} + K_{needle}$, the relation becomes too steep, which means that emptying could become sensitive to production tolerances.

2.3. Experimental set-up

2.3.1. Flow facilities and instrumentation

Two different set-up were used for the present work. The first set-up was built to conduct experiments with up-scaled prototypes in water. In this set-up, fluid and particle flow visualizations, particle emptying experiments and pressure drop measurements were carried out. The second set-up was built to conduct emptying experiments with real blisters and real particles in air.

The set-up for up-scaled prototypes is an open loop constant overhead water channel (Wachtel et al., 2008). The flow facility and instrumentation are shown in Fig. 7. The fresh water is continuously supplied to the flow facility through a deaeration filter. The water height in the facility is kept constant by draining the overflow. The inhaler model, preferably 5× upscaled, is connected to a 5× upscaled USP throat (United States Pharmacopeia, 2000).

The flow rate of the system is adjusted using a needle valve and measured by three serially connected rotameters having ranges of 5–50, 30–300 and 100–1000 l/h, which enables flow rates in the ranges 5–1000 l/h to be set with the same relative accuracy. The pressure drop across the inhalers or the components of the inhalers are measured by three differential pressure transducers connected in parallel. The transducers have different measurement ranges, and as a consequence of parallel connection, the measurement accuracy is kept constant in a wide range of flow rates. Two pressure taps (Fig. 8) are used; one of them is inserted after the mouth piece and the second one is open to the ambient, so that the pressure difference along the inhaler can be measured.

The main objective of emptying experiments is to determine the minimum flow rate at which complete emptying of particles from the blister takes place. The blisters are filled with model particles and the flow rate is adjusted with the aid of a needle valve and flow rate meters. The flow rate is gradually increased until complete emptying is achieved. This flow rate is recorded as the minimum flow rate for emptying. During this procedure, the particle flow rate is recorded with a video camera. The flow and particle visualization studies were performed by injecting ink of different colors into the models. Two syringe pumps were used for accurate adjustment of the ink flow rate. Depending on the flow velocity, two different video-cameras are used: Sony HDV1080i camcorder recording at 25 fps, and Weinberger Visario high-speed camera recording at max 10,000 fps. Blister emptying experiments, for example, are recorded by Sony HDV1080i. The results of the flow visualization studies are not reported here but they are basically used to understand the character of the flow in

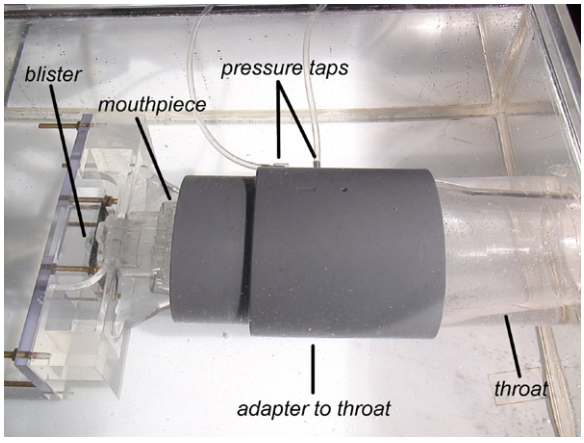

Fig. 8. The upscaled transparent prototype of an inhaler in the water channel.

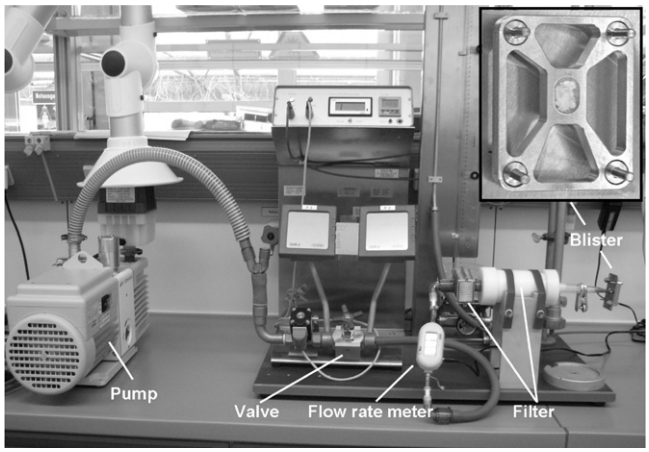

Fig. 9. The set-up of emptying experiments conducted with real blister models and particles.

the DPI and, accordingly, initiate appropriate modifications on the components.

Second set-up is built to conduct emptying experiments from the real blister geometries (Fig. 9). Only a small number of selected blister models were tested in this test-rig. After the blister has been filled with a specified quantity of powder, it is closed with the lid foil containing the pierced holes.

The air is drawn through the blister. The flow rate is set with the aid of a valve and measured using a flow rate meter. Upstream of the flow rate meter, particle-laden flow is filtered. Flow rate is gradually increased till complete emptying is achieved. For each flow rate, the amount of emptying is measured by weighing the blister.

2.3.2. Selection of test particles

Particles with a diameter of 200 μm and a density of 1050 kg/m^3 are required for experiments under full similarity conditions in a 5× upscaled model in water. Unfortunately, particles having exactly this density are difficult to find. If particles with a larger diameter and/or density are selected, the experiments will not satisfy the similarity conditions at particle level. Having said that, denser particles can still be selected on the assumption that each blister has a Re_p^*–Ar curve akin to channels and pipes as per Fig. 3. For a specific particle and a specific flow rate through the blister, the particles can be in either pickup or non-pickup regime. As the Ar is proportional to the particle density ρ_p, a horizontal shift to the right in the Re_p^*–Ar diagram can be achieved by using denser particles, providing that the particle diameter is kept constant. A vertical shift in the Re_p^*–Ar diagram can be achieved by changing the flow rate. Hence, if particle emptying for a specific blister occurs at the selected Ar number and Re_p (flow rate), this blister can be emptied at the same Re_p under full similarity conditions. The advantage of using denser particles is a longer blister emptying time, which can be measured with greater confidence. This information will help to adjust the total flow resistance coefficient of the inhaler to a defined target value. As particles satisfying the full similarity conditions are difficult to find, we have chosen PMMA particles as representative of real conditions. The selected PMMA particles have a mean particle diameter of 200 μm and a density of 1190 kg/m^3. As can be seen in Re_p^*–Ar plot in Fig. 3, these particles create conditions which most closely approximate reality. In order to simulate a poor-case emptying scenario, iron particles having a 300 μm mean diameter are employed. All the particle types used in the present investigations are listed in Table 1 and their Ar values are depicted as vertical lines in Fig. 3.

Table 1
The properties of the particles used (see also Fig. 3).

Material	Density [kg/m^3]	Size [μm]	Ar (in water)
Lactose	1540	40	3.3
PMMA	1190	150–250	6–28
Iron	7870.0	150–450	223–6020

3. Results and discussion

3.1. Experimental characterization of blisters

3.1.1. Flow rate for complete emptying of particles

In order to compare the emptying performance of the blisters, the minimum flow rates at which complete emptying of the particles from the blister was achieved were measured. Blisters emptied at lower flow rates are rated better than those emptied at higher flow rates. The minimum flow rates at which emptying was achieved were determined by visualizing particle movement during emptying at constant flow rates. Specimen images from particle visualizations recorded during blister emptying are shown in Fig. 10. This kind of visualization, in addition to determining flow rates required for emptying, also provided valuable information on dead flow regions and thus aided selection of the most appropriate location for the inlet holes in the blister. One important finding to emerge from the visualization studies is that continuous emptying of the particles leads to unsteady flow within the blister.

The emptying experiments were conducted with PMMA and iron particles. A comparison of various blisters tested is provided in Fig. 11. Note that, the measured water flow rates are converted to corresponding air flow rates by using Eq. (11). As experiments with PMMA particles giving an Ar of 17 are the closest to full similarity in respect of the actual application conditions, the final ranking should be made based on these experiments. Fig. 11 shows that, for most of the tested blisters complete emptying can be achieved under 10 l/min. As Fig. 6 shows, this flow rate is in a region where the flow resistance coefficients of the components have least sensitivity to one another. We therefore set a flow rate of 10 l/min through the blister as the upper limit. It should be noted that the major geometrical difference between 5c and 6c is the larger projection area and volume of 6c. Thus, 6c preferable to 5c as it provides more volume for the drug powder. It was subsequently decided that the outlet of the blister, which simultaneously functions as the inlet of the needle, should be connected to the upper hole of the blister to avoid inhalation of a lumps of powder which could escape into the mouth piece just after the blister has been pierced prior to inhalation. Nevertheless, in order to assess the effect of the mouthpiece location on emptying, all 2bb models were tested using two different inlet locations. 2bb models were tested using two different inlet locations. The blisters designated as “reversed” in Fig. 11 are those in which the outlet of the blister was connected to the lower hole of the blister so that particles were transported in the direction of gravity. Although the tests carried out using PMMA particles provide a valid comparison between different blisters, it was decided to verify the results by performing measurements using iron particles. Particles with a maximum diameter of 450 μm and a mean diameter of 300 μm were selected in order to increase the Ar and achieve a shift both in Re_p^* and Ar shift in the Re_p^*–Ar diagram for a particular blister. The results of the tests with the iron particles are compared with the results of the tests with the PMMA particles in Fig. 11. The ranking of the blisters is slightly different for the iron particles but it should be noted that, even for these very dense particles, the flow rates required for emptying are lower than 10 l/min for blisters 5c,

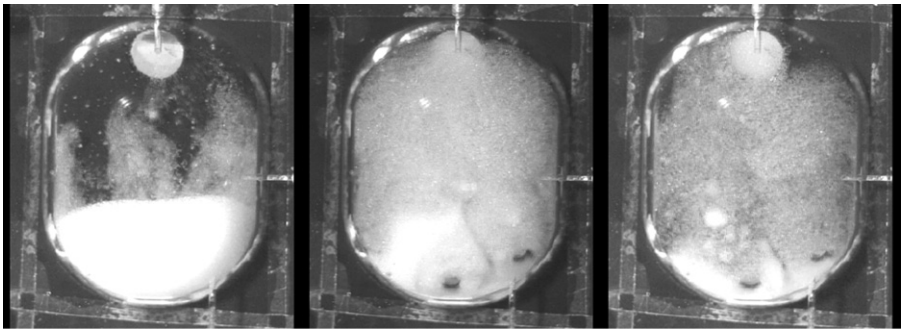

Fig. 10. Snapshots from the visualizations of PMMA particle emptying.

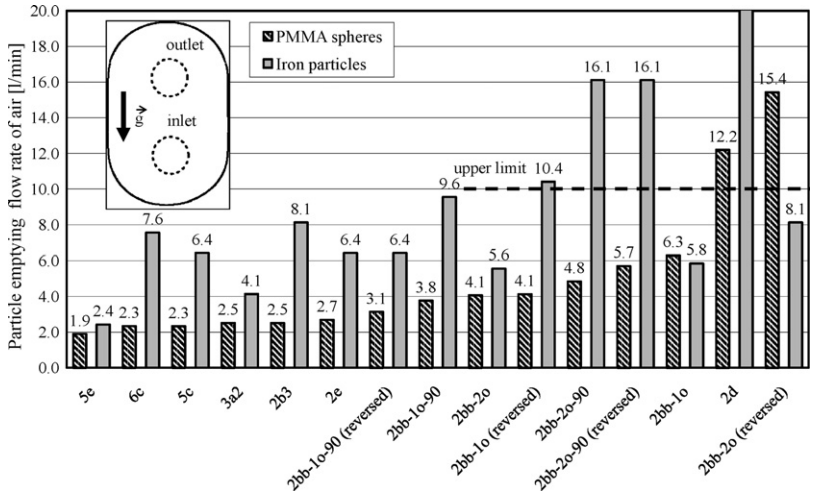

Fig. 11. Comparison of minimum flow rates required for emptying of PMMA and iron particles. Longer blister axis is parallel to direction of gravity. Upper hole kept as outlet of the blister, except in "(reversed)" cases, where lower is the outlet.

6c, 5e, 3a2, 2b3 and 2e. Flow rates lower than 10 l/min offer flexibility both in blister selection and in the modifications that can be made to the other parts of the inhaler. For some of the blisters selected (2b3, 2e), emptying experiments were conducted with 1× scaled models using lactose particles having a mean diameter of 40 μm.

As can be seen in Fig. 12, the flow rates for complete emptying in 1× scaled models are consistent with the minimum flow rates for emptying determined in the upscaled water experiments. This clearly indicates that the experimental procedure used, which is conducted in water with upscaled models and particles, is sufficiently accurate to give valid blister emptying data.

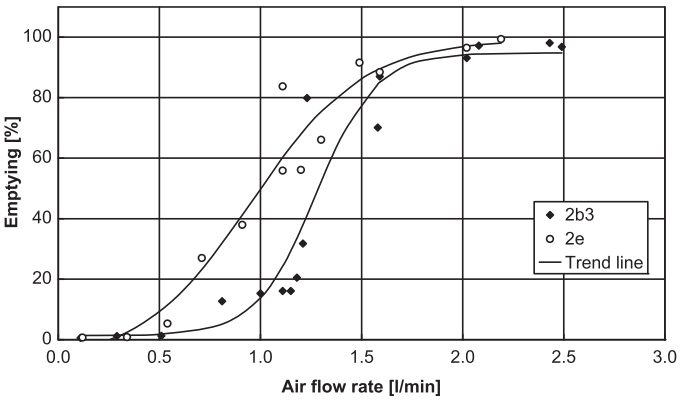

Fig. 12. Particle emptying tests conducted with 1× scaled blister models.

3.1.2. Flow resistance of the blisters and the other components of the inhaler

In order to match the blisters with the other components of the inhaler over the range of flow rates within which the patient can completely empty the blister, it is essential to know the flow resistance characteristic of each blister. In subsequent step, therefore, the flow resistance characteristics of all blisters and the other components of the inhaler were measured in the water channel and then converted to flow resistance characteristics in air using the relevant conversion factors (Section 2.2.1). The measurements made for 2b3 + needle, which has been converted to relevant values in air, is shown in Fig. 13a as an example.

As illustrated in Fig. 13b, the pressure drop is linear function of the Q^2, as stated by Eq. (13). All blisters and other components of the inhaler showed similar linear behaviour. Hence, the flow resistance characteristic of each component is going to be represented by the factor K. In Fig. 14, the K of all blisters, the 10 mm i.d. needle and the initial bypass opening are shown. It should be noted that all measurements carried out on blisters had to be performed in conjunction with the needle; the results therefore represents total pressure drop for the blister and the needle. As the blisters and the needle serially connected, the measurements yielded a value for $K_{blister} + K_{needle}$. The measurement of K_{needle} alone enabled us to determine the actual pressure drop for the blister.

Evaluating Fig. 14 together with Fig. 11, it can be seen, not surprisingly, that all blisters performed well, apart from 5e and 2e, have high pressure resistance coefficients. This was expected as particle emptying requires high flow velocity, but the pressure drop increases with the square of the flow velocity. In other words, most of the blisters require lower flow rates have to empty them

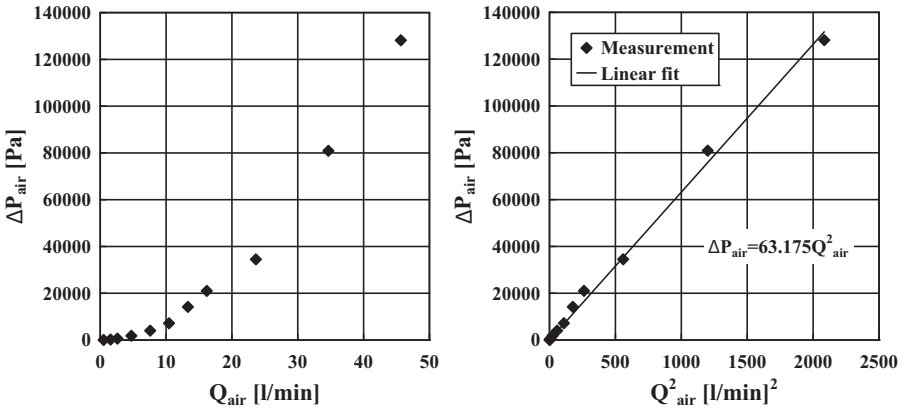

(a) $\Delta P - Q$ characteristic (b) $\Delta P - Q^2$ characteristic

Fig. 13. The measured flow resistance characteristics of the components 2b3 + needle. Values are given for air.

have higher local internal flow velocities. It is still possible, however, to modify the inlet and outlet geometries of the blisters in order to reduce the pressure drop across them without an unacceptable reduction in their emptying performance. These issues are addressed in the subsequent sections. At this point, therefore, the first five steps of the suggested design method are complete. The remaining steps focus on the optimization of the existing prototypes of the components with a view to ensuring that the new DPI satisfies the performance requirements.

3.2. Optimization process

In Fig. 15a, the design line and the initial state for the bypass + 2b3 + needle combination are plotted. This combination results in a $K_{inhaler}$ value of 7.96, which is much higher than the target value of 2.62. In Fig. 15b, the flow rate through the blister for a $K_{inhaler}$ value of 2.62 is plotted together with the flow rates required for emptying for 2b3 and the initial state of the bypass + (2b3 + needle) combination. As discussed previously, $K_{blister} + K_{needle}$ should be reduced to 10 so that $Q_{blister}$ reaches values around 10 l/min, which is the same flow rate as through the bypass opening. The flow rates through the blister and the bypass opening were selected to be equal because, in this condition, as can be seen from Fig. 6, the flow rates are relatively insensitive to changes in the flow resistances of the bypass opening, the blister and the needle. Selecting similar values for the bypass and blister flow rates eliminates over-stringent production tolerances and reduces production costs. Therefore, the target for optimization should be reduction of the K value of the 2b3 (or any other blister) + bypass + needle combination, achievable by modifying the geometries of the individual components so that $K_{inhaler}$ is 2.62 and $Q_{blister}$ is 10 l/min, giving a total flow rate of Q_T = 20 l/min.

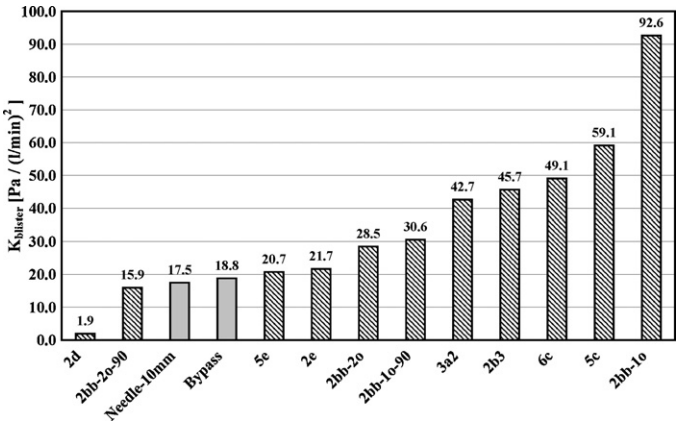

Fig. 14. Comparison of pressure resistance coefficients (K) of the 10-mm i.d. needle, the bypass and various blisters (valid for air flow).

Any modification to the blister must ensure the flow rate required to achieve emptying is kept below 10 l/min. In order to achieve this target, the geometries of the blister, needle and bypass were systematically modified and measurements of K values and flow rates for emptying were performed in order to verify the modifications. Optimization can be accomplished in three parts: optimization of the blister, optimization of the bypass opening and optimization of the needle.

The critical components of the inhaler, which should match one another, are therefore the blister, the bypass and the needle, and it is these components which principally determine the resultant $K_{inhaler}$ value. The pressure resistance coefficient of the blister, bypass and needle combination is:

$$K_t = \frac{(K_{blister} + K_{needle})K_{bypass}}{K_{blister} + K_{needle} + K_{bypass} + 2\sqrt{(K_{blister} + K_{needle})K_{bypass}}} \quad (18)$$

As the blister is the most critical component of the DPI as a whole, optimization started with the modification of a selected blister. On the basis of the measurements carried out, blister 2b3 was selected because of its general shape and large volume. Although it has optimal emptying performance and a relatively simple geometry, its flow resistance coefficient is very high. The diameters of the inlet and outlet holes are the main dimensions that influence the flow resistance and it was therefore these parameters that were varied during the optimization process. The dimensions of the needle and the bypass were the other parameters that were optimized to achieve the design goals. It was shown in Section 2.2.2 that matching the bypass with the blister and needle is particularly important because the flow rate in the blister is directly related to drug emptying.

In view of the above considerations, pressure resistance coefficients (K) were calculated for each component of the new DPI in order to achieve the design goals defined earlier. These coefficients are presented in Table 2. Each component was then optimized separately to obtain the target values listed in Table 2. The procedure is necessarily iterative, however, because there is no analytical way in which the flow resistance and the flow rate required for emptying of the blister can be related to the sizes of the blister holes. Emptying flow rate and flow resistance experiments therefore had to be performed after every change in the dimensions of the holes. Nevertheless, after several iterations, the initial geometry evolved to its

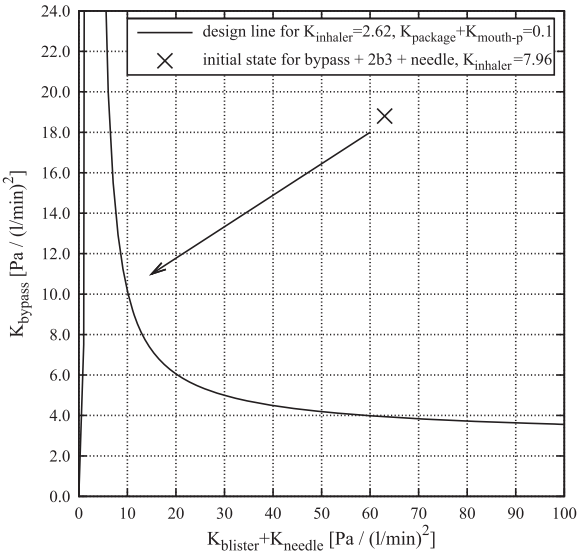

(a) Relationship between K_{bypass} and $K_{needle} + K_{blister}$

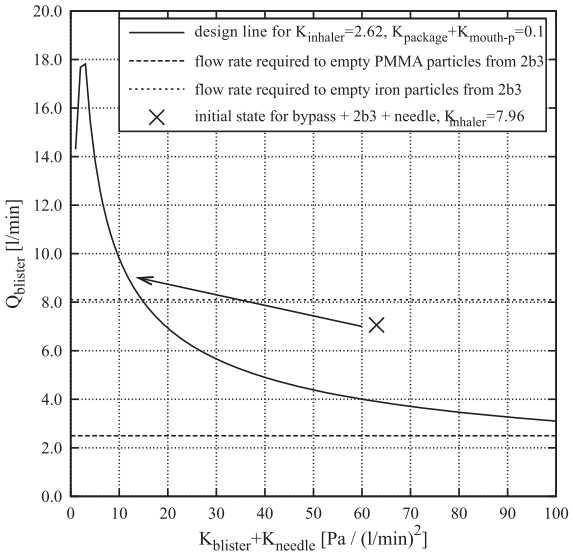

(b) Relationship between $Q_{blister}$ and $K_{needle} + K_{blister}$

Fig. 15. Design point selection, taking into account both aerodynamic and particle emptying constraints.

Table 2
Target, initial and final pressure resistance coefficients for various components of new DPI with blister model 2b3.

Components	Target K	Initial K	Final K
Blister	10	45.7	10.3
Needle	5	17.5	6.3
Bypass	7	18.8	7.5
Package + mouthpiece	~0.1	–	–
Inhaler	2.62	8.0	2.3

Table 3
Pressure resistance coefficients and flow rates required to empty initial and final blister models 2b3.

Performance parameters	Initial 2b3	Final 2b3
$K_{blister}$ (Pa/(l/min))	63.23	10.3
Flow rate required to empty PMMA particles (l/min)	2.6	2.6
Flow rate required to empty iron particles (l/min)	8.1	10.0

final form. The pressure drop vs. flow rate curve for the initial and final blister geometries is shown in Fig. 16 and the corresponding K values and flow rates required for emptying of the blisters are listed in Table 3. As can be seen from Tables 2 and 3, the target K value was reached in the final version without significant changes in the flow rate required for emptying. The same type of iterative procedure was used for needle and bypass optimization and here, too, the selected K values were achieved (Table 2). Fig. 17 shows the pressure drop characteristics of the HandiHaler®, the Respimat® and the new DPI. The new DPI resembles the HandiHaler® in terms of its flow resistance characteristics although it deviates at higher volume flow rates and shows non-linear behaviour. This behaviour is most probably due to a flow regime change inside the DPI at higher flow rates.

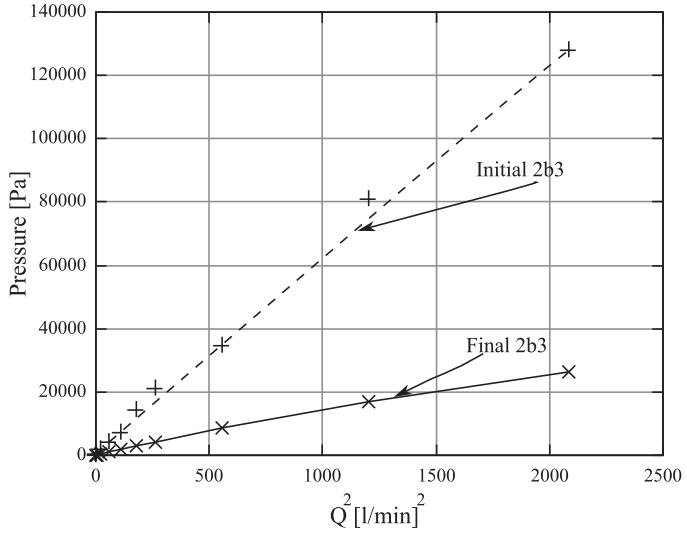

Fig. 16. Pressure drop vs. flow rate curves for the 2b3 blister before and after optimization.

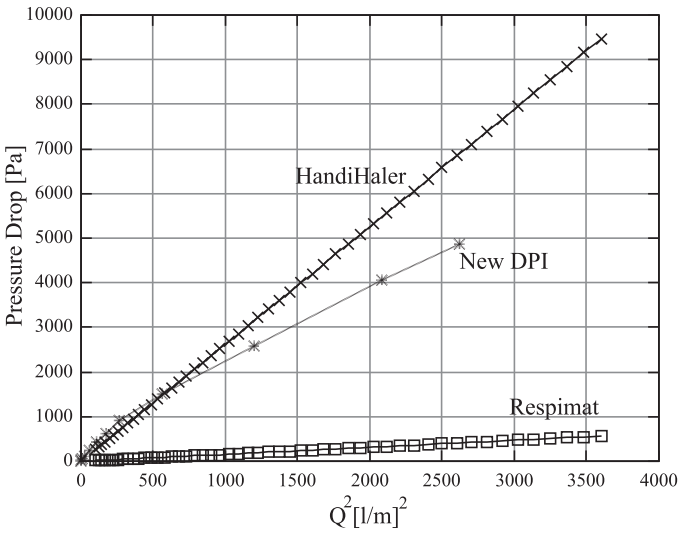

Fig. 17. The pressure drop characteristics of the various inhalers.

4. Conclusions and outlook

A design methodology was developed and applied to design and optimize a DPI. The new DPI was tested and shown to meet the design goals. The measurement method used, which employed upscaled models of inhaler and particles in water, was validated by the emptying experiments conducted with real blister geometries in air. An analytical flow resistance model was established and its usage, together with a series of emptying experiments, was presented.

With the aid of the design methodology presented here, the overall design cycle time for a DPI can be reduced. Nevertheless, inhaler performance cannot be judged solely on emptying and flow resistance considerations. Particle deposition in the inhaler and the mouth-throat region of the patient is important and must be considered carefully. Powder formulation and the dispersion performance of the powder agglomerates of inhaler have huge impact on drug delivery. Particle size distribution after the inhaler with actual powder formulation should be tested and the inhaler and/or the powder formulation should be modified if necessary. Another important factor on deposition is the inhaler exit velocity. Higher inhaler exit velocities have a marked effect on particle deposition in the mouth-throat region (Grgic et al., 2004). In our design perspective, preference should be given to lower exit velocities. However, deposition tests should be performed before finalizing the device design.

Acknowledgments

The authors acknowledge the financial support given by Boehringer Ingelheim Pharma GmbH & Co. KG. The authors are also grateful to David Parker for making the necessary English corrections required in the paper.

References

Ashurst, B., Malton, I., Prime, A., Sumby, D., 2000. Latest advances in the development of dry powder inhalers. Pharmaceutical Science and Technology Today 3, 246–256.

Breuer, M., Baytekin, H., Matida, E., 2006. Prediction of aerosol deposition in 90° bends using LES and an efficient Lagrangian tracking method. Journal of Aerosol Science 37, 1407–1428.

Breuer, M., Matida, E., Delgado, A., 2007. Prediction of aerosol drug deposition using an Eulerian–Lagrangian method based on LES. In: The Proceedings of 6th International Conference on Multiphase Flow (ICMF 2007), Leipzig, Germany, p. S7 Tue B 20.

Chodosh, T.J., Flanders, S., Kesten, J., Serby, S., Hochrainer, C., Chodosh, D.W.J., 2001. Effective delivery of particles with the HandiHaler® dry powder inhalation system over a range of chronic obstructive pulmonary disease severity. Journal of Aerosol Medicine: Deposition, Clearance, and Effects in the Lung 14, 309–315.

de Boer, A., Winter, H., Lerk, C., 1996. Inhalation characteristics and their effects on in vitro drug delivery from dry powder inhalers: Part 1. Inhalation characteristics, work of breathing and volunteers' preference in dependence of the inhaler resistance. International Journal of Pharmaceutics 130, 231–244.

Grgic, B., Finlay, W., Burnell, P., Heenan, A., 2004. In vitro intersubject and intrasubject deposition measurements in realistic mouth-throat geometries. Journal of Aerosol Science 35, 1025–1040.

Islam, E., Gladki, N., 2008. Dry powder inhalers (dpis) – a review of device reliability and innovation. International Journal of Pharmaceutics 360, 1–11.

Kalman, H., Satran, A., Meir, D., Rabinovich, E., 2005. Pickup (critical) velocity of particles. Powder Technology 160, 103–113.

Larock, B.E., Jeppson, R.W., Watters, G.Z., 1999. Hydraulics of Pipeline Systems, 1st edition. CRC Press.

Licalsi, C., Christensen, C., Bennett, T., Phillips, J., Witham, E., 1999. Dry powder inhalation as a potential delivery method for vaccines. Vaccine 17, 1796–1803.

Owens, G., Zinman, D., Bolli, B., 2003. Alternative routes of insulin delivery. Diabetic Medicine 20, 886–898.

Patton, R., Trinchero, J., Platz, P., 1994. Bioavailability of pulmonary delivered peptides and proteins: α-interferon, calcitonins and parathyroid hormones. Journal of Controlled Release 28, 79–85.

United States Pharmacopeia, 2000.

Wachtel, H., Ertunç, Ö., Köksöy, Ç., Delgado, A., 2008. Aerodynamic optimization of handihaler and respimat: the roles of computational fluid dynamics and flow visualization. In: Respiratory Drug Delivery, Scottsdale, Arizona, USA, pp. 165–174.